

Computational mechanistic study of copper-catalysed tandem arylation-cyclization reaction of alkynes and diaryliodonium salts

Tamás Károly Stenczel¹, Ádám Sinai,^{2,3} Zoltán Novák*² and András Stirling*⁴

Address: ¹Török Ignác Secondary School, Gödöllő, Hungary, Present address: St Catharine's College, Cambridge CB2 1RL, UK

² ELTE "Lendület" Laboratory of Catalysis and Organic Synthesis, Eötvös Loránd University, Institute of Chemistry, Budapest, Hungary.

³ Servier Research Institute of Medicinal Chemistry, Záhony utca 7. H-1031, Budapest, Hungary

⁴ Research Centre for Natural Sciences of the, Hungarian Academy of Sciences, Institute of Organic Chemistry, Budapest, Hungary.

Email: Zoltán Novák – novakz@elte.hu; András Stirling - stirling.andras@ttk.mta.hu

* Corresponding author

Abstract

We present a computational mechanistic study on the copper(III) catalysed carboarylation-ring closure reactions leading to the formation of functionalized heterocycles. The calculations considered two viable options for the underlying mechanism which differ in the order of the oxazoline ring formation and the aryl transfer steps. In our model transformation, it was found that the reaction generally features the aryl transfer - ring closing sequence and this sequence shows very

limited sensitivity to the variation of the substituent of the reactants. On the basis of the mechanism the origin of the stereoselectivity is ascribed to the interaction of the Cu ion with the oxazoline oxygen driving the ring closure step selectively.

Keywords

catalysis; DFT calculation; iodonium salts; reaction mechanism; tandem arylation-cyclization

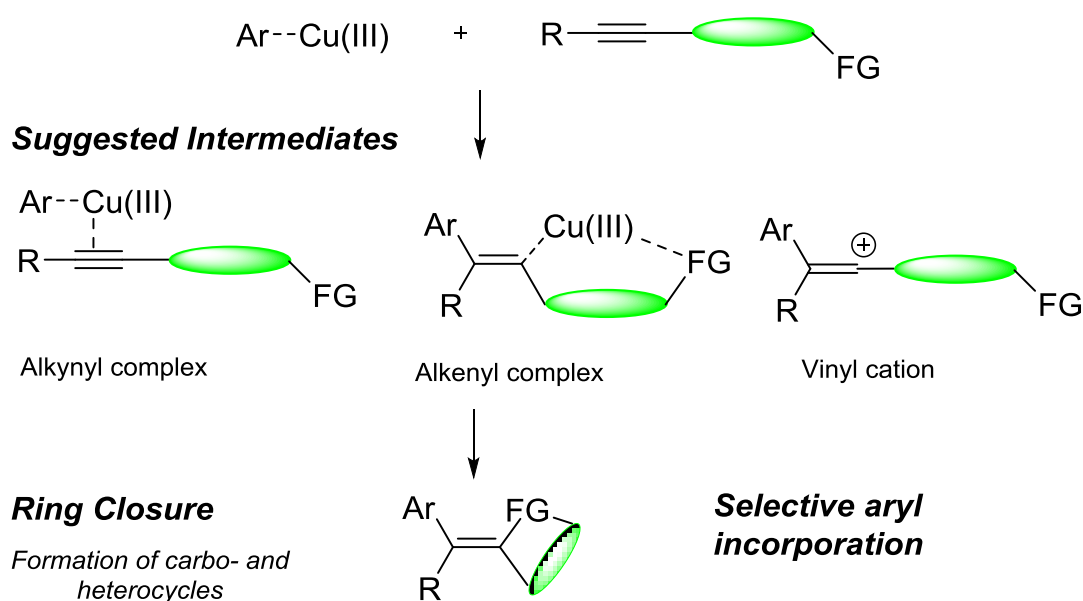
Introduction

Recently a very efficient synthetic strategy has been developed where diaryl iodonium salt [1-8] and Cu-compounds are employed together to produce in-situ Cu(III)-containing aromatic electrophile equivalents which then play crucial role in carbofunctionalization processes [9-28]. In particular, tandem arylation-cyclization reactions promoted by the postulated highly electrophilic Cu(III)-aryl intermediates can allow access to aryl functionalized carbocyclic and heterocyclic molecules with valuable functionalities [9, 29-43]. The mechanistic details of these cascade reactions are not clear as evidenced by the different mechanistic proposals (see e.g. Refs. 18, 30, 40, and 44) These mechanisms suggest the presence and existence of vinyl cation or alkynyl-Cu(III), alkenyl-Cu(III) complexes before the C-O bond formation in the ring closing step (see Scheme 1).

As an example of the catalytic arylation-cyclization strategy, an efficient procedure to form substituted oxazoline derivatives from alkyl- and aryl-propargylamides has been developed, where the process involves a 5-exo-dig cyclization and an aryl group transfer steps affording a wide range of oxazoline derivatives [44]. An intriguing issue is the order of the arylation and ring closure steps and whether this sequence can be

affected by the electronic or steric properties of the ligands. Clearly this issue is also interesting for other, analogous copper catalysed arylation-cyclization reactions. Although these mechanistic variations have been postulated in the literature, the exact sequence remained unclear. In this study we report our theoretical study addressing the mechanism of this reaction.

Reaction of Ar-Cu(III) and alkyne



FG: Lewis basic or nucleophilic Functional Group

 : linker containing carbon and heteroatom

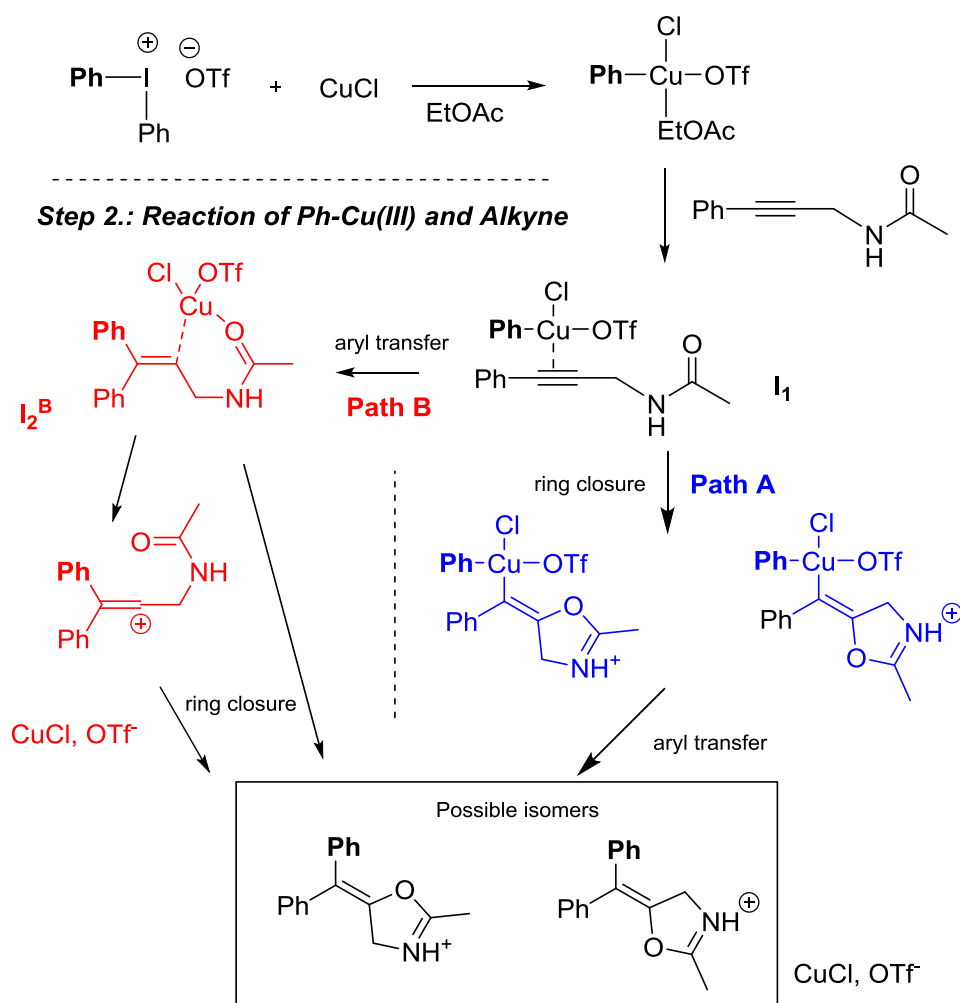
Scheme 1: Possible intermediates of the interaction of alkyne compounds and Ar-Cu(III) species.

Results and Discussion

First, we explain our computational strategy and discuss the possible reaction paths leading to the formation of 5-(diphenylmethylene)-4,5-dihydrooxazole in the reaction of propargylic amides and diaryliodonium salts in the presence of Cu(I) catalyst. This is a simplified model of the original reaction scheme [44] and allows the exploration of the possible reaction routes of the carbonylation-ring closure reactions in a

computationally efficient manner. As the first step of the reaction we considered the formation of the key Ar-Cu(III) species, followed by the interaction of this intermediate with the alkyne (Scheme 2. Step 1.). In the next step we compared the energetics of two different paths (Path A and B), to get insight into the order of the arylation and cyclization steps. Additionally, the relevance of vinyl cation formation and the stereoselectivity were examined.

Step 1.: Formation of Ph-Cu(III) species



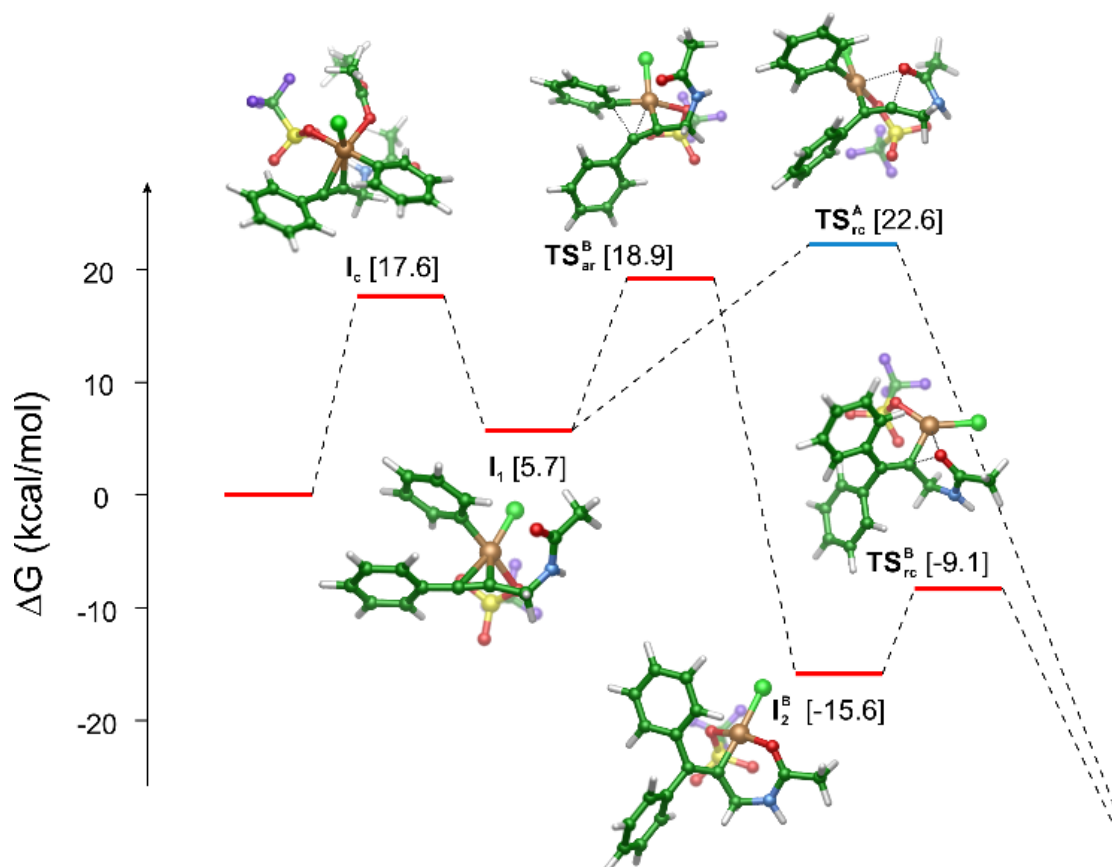
Scheme 2: Two possible reaction routes for the oxazoline formation explored by computations. The schemes indicate the possible stereochemical outcomes.

The energy profiles start with the interaction of the reactant with the catalyst complex formed in the EtOAc medium. In this process the complexing EtOAc ligand leaves and the reactant N-(3-phenylprop-2-yn-1-yl)acetamide binds to the Cu(III) ion in an η^2 mode with its triple bond. The process occurs following an associative substitution fashion often observed for the 16e metal complexes. We could locate a crucial structure where the incoming reactant and the leaving solvent molecule occupies the equatorial position of the trigonal bipyramid formed by the five ligands of the Cu(III) ion. We decided to characterize this step by the free energy level of the intermediate: 17.6 kcal/mol (I_c). There are two reasons behind this choice: i) the preceding and subsequent barriers were computed to be very close in energy to that of this structure; ii) one of the participants of this step is the solvent EtOAc molecule, ie. the solvent plays a two-fold role: it is a reactant and a solvating agent; as it is known, such situations are difficult to describe by implicit solvent models [45]. The intermediate formed in this step (I_1) is stabilized at 5.7 kcal/mol.

From this intermediate the two reaction paths diverge. On path A (blue in Scheme 2 and 3) the ring formation takes place with an activation free barrier of 22.6 kcal/mol (TS_{rc}^A). Along this path this is the rate determining step. The calculations revealed that once the ring is formed the aryl transfer spontaneously occurs and a significant free energy is released (more than 70 kcal/mol) by the formation of the adduct of the protonated product and the catalyst (free energy level of -50.5 kcal/mol).

In contrast the route starting with the aryl transfer from Cu(III) to the activated reactant features a two-step mechanism (red in Scheme 2 and 3): the aryl-transfer leads to the formation of a quite stable intermediate I_2^B with a ca. -20 kcal/mol exergonicity with respect to the first intermediate. We can also notice that this step requires a smaller, 18.9 kcal/mol activation free energy (TS_{ar}^B) as compared to TS_{rc}^A . The aryl transfer is followed by the O-C bond formation which results in the oxazoline

ring. This step requires a moderate 6.5 kcal/mol activation energy (TS_{rc}^B) which indicates that this step is very fast under the reaction conditions. After the ring is formed the system is stabilized by releasing a large amount free energy to arrive at the same state as postulated for path A.



Scheme 3: Free energy profiles for the possible reaction routes. The final energy state (-50.5 kcal/mol) is not shown. Red: first the aryl transfer occurs followed by the oxazoline ring closure; blue: ring closing takes place first followed by spontaneous aryl transfer. The dashed lines are only guides to the eyes. Colour code for the structures: green: C; red: O; light green: Cl; blue: N; yellow: S; violet: F; bronze: Cu.

Comparison of the two free energy profiles indicate that the preferred route is the one where the aryl transfer precedes the oxazoline ring formation. On the other hand, the calculated activation free energy barriers are compatible for both routes with the

experimental conditions and indicate that both mechanisms can operate at the relatively low, 50°C temperature.

As the reaction profiles indicate the final state is highly stable. Further stabilization is expected when the product is formed by deprotonation (presumably at the workup stage). However, deprotonation may occur earlier if this is thermodynamically favorable in the presence of a suitable base. In the reaction mixture such potential bases are the triflate anion and the reactant. As they are very weak bases we can expect that deprotonation does not take place before the final product formation. Indeed, the calculations show that none of the reactants and intermediates are strong enough acids to deprotonate: +55 kcal/mol, +18 kcal/mol and +25 kcal/mol of free energy are required to deprotonate the reactant and intermediates I_1 and I_2^B , respectively.

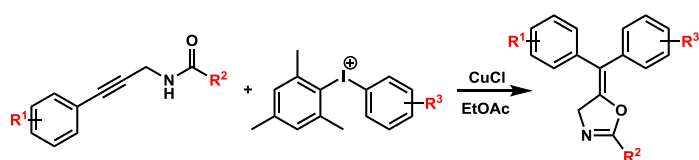
As Scheme 2 indicates the products oxazoline can be cis or trans isomers regarding the relative positions of the oxazoline oxygen and the incoming aryl group at the double bond. Formation of a vinyl cation would imply a non-stereospecific oxazoline formation. The calculations however revealed that its formation requires ca. 3 kcal/mol more free energy investment than the barrier toward the intramolecular ring closure. Therefore, we can exclude that the reaction path goes through a vinyl cation intermediate. In contrast, the mechanism obtained from the calculations shows that the catalyst steadily interacts with the substrate via Cu-C bonds along the full path. Further inspection reveals a crucial interaction between the carbonyl oxygen and the catalyst Cu ion (see e.g. I_2 in Scheme 3 where the Cu-O bond length is 1.87Å). In fact, this cooperation drives selectively the reaction toward the formation of the cis isomer, which is consistent with the experimental results.

Although the above 3 kcal/mol energy difference is large enough to guide the reaction toward the intermolecular ring closure, it is important to note that this also

indicates an opportunity to influence the reaction mechanism: stabilization of the vinyl cation [17,42] may induce a deviation toward a path with less efficient stereocontrol.

To obtain further insight into the mechanism we have calculated these paths for a large number of reactions where the R¹, R² and R³ substituents of the reactants are varied (see reaction scheme in Table 1). A selection of these routes is summarized in Table 1 whereas the data of the full set of reactions are given in the Supporting Information. The reactions collected in Table 1 represent the scope of the methodology [44]. Inspection of Table 1 shows that the aryl transfer route is always preferred to the one where the oxazoline ring formation occurs first (the barriers of the ring closure are consistently higher than those of the aryl transfers). It is also interesting to note that in some cases the initial complex formation is the rate determining step along the aryl-transfer path although in most cases the differences in the two barrier heights are very small.

Table 1: Effect of the substituents on the barrier heights (kcal/mol). Selection of the substituents are based on Ref. 44.



| R ¹ | R ² | R ³ | barrier of (kcal/mol) | | |
|--------------------|-------------------------------|-----------------|-----------------------|---------------------|--------------------|
| | | | complex formation | aryl transfer first | ring closure first |
| Ph | <i>t</i> -Bu | Ph | 16.9 | 17.6 | 19.8 |
| <i>o</i> -Me-Ph | <i>t</i> -Bu | Ph | 19.4 | 18.8 | 21.3 |
| <i>p</i> -Me-Ph | <i>t</i> -Bu | Ph | 15.4 | 17.5 | 20.9 |
| <i>p</i> -OMe-Ph | <i>t</i> -Bu | Ph | 15.8 | 17.7 | 20.3 |
| <i>p</i> -COOEt-Ph | <i>t</i> -Bu | Ph | 18.5 | 18.8 | 21.7 |
| <i>p</i> -Ac-Ph | <i>t</i> -Bu | Ph | 18.6 | 18.9 | 20.3 |
| <i>p</i> -Cl-Ph | <i>t</i> -Bu | Ph | 16.6 | 17.8 | 19.1 |
| <i>m</i> -Br-Ph | <i>t</i> -Bu | Ph | 17.0 | 18.7 | 20.3 |
| Ph | Ph | Ph | 16.5 | 18.5 | 21.9 |
| Ph | <i>p</i> -MeO-Ph | Ph | 12.3 | 11.8 | 16.1 |
| Ph | <i>p</i> -NO ₂ -Ph | Ph | 17.0 | 19.5 | 23.9 |
| Ph | <i>t</i> -Bu | <i>m</i> -Br-Ph | 18.8 | 17.1 | 19.4 |
| Ph | <i>t</i> -Bu | <i>p</i> -Ac-Ph | 18.1 | 17.6 | 18.8 |
| 2-Thiophene | <i>t</i> -Bu | Ph | 16.9 | 18.5 | 18.5 |
| Ph | Et | Ph | 18.0 | 18.6 | 21.0 |
| Et | <i>t</i> -Bu | Ph | 17.9 | 17.2 | 19.5 |

The full set of reactions also shows that the aryl transfer as the first step after the complex formation with the catalyst is preferred over the route where the ring closure precedes the aryl transfer. Only three cases from the calculated ca. fifty reactions show a reverse trend. We could not identify a common motif behind this discrepancy, instead we attribute these exceptions to the limitations of the methodology.

Conclusion

In summary, we have shown with the selected model reaction that the above copper-catalysed carboarylation-ring closure reaction of alkynyl substrates with diaryliodonium salts can be depicted as follows: first the Cu(III)-aryl electrophile forms an intermediate with the triple bond of the reactant, then the aryl moiety migrates to the activated triple bond which is followed by a fast ring closing step. The calculations provided several new chemical insights: deprotonation can take place only after the tandem arylation-cyclization sequence; the mechanism shows a very limited sensitivity in a wide range of substituents installed on the reactants; a crucial copper-oxygen interaction is responsible for the very high stereoselectivity of the reaction and it also excludes the formation of vinyl-cation intermediates. The obtained results could serve as useful and more general description of the mechanism of the carboarylation-ring closure strategy based on the utilization of alkynes and diaryliodonium salts, beyond the selected and studied oxazoline synthesis.

Experimental

The calculations have been performed using the Gaussian 09 program package [46]. The M06 exchange-correlation functionals have been employed to solve the Kohn-Sham equations [47]. For the geometry optimizations, transition state searches and

vibrational calculations the 6 31G* basis set has been used. All the stationary structures obtained by the optimization procedures were further recalculated using the 6 311++G(3df,3pd) basis set and the SMD implicit solvent model employing ethyl acetate as solvent [48]. The equilibrium structures of the reactant, product and intermediate states had only positive frequencies. The transition states have been verified having a single imaginary frequency and connecting the corresponding intermediate structures. The discussions are based on Gibbs free energies obtained within the ideal-gas model using the rigid-rotor harmonic-oscillator model for 323.15 K (experimental condition).

Supporting Information

Full version of Table 1, total energies and Cartesian coordinates of all stationary points (PDF).

Supporting Information File 1:

File Name: BJOC_SupportingInformation_File1

File Format: pdf

Acknowledgements

This work was supported by NKFI (Grant No. K116034 and K125020). This project was supported by the János Bolyai Research Scholarship of the Hungarian Academy of Sciences.

References

1. Stang, P. J.; Zhdankin, V. V.; Tykwinski, R.; Zefirov, N. S. *Tetrahedron Lett.* **1992**, *33*, 1419–1422.
2. Merritt, E. A.; Olofsson, B.; *Angew. Chem. Int. Ed.* **2009**, *48*, 9052–9070.
3. Bouma, J. M.; Olofsson, B. *Chem. Eur. J.* **2012**, *18*, 14242–14245.
- 4.(d) Bielawski, M.; Olofsson, B. *Chem. Commun.* **2007**, *25*, 2521–2523.
5. Yusubov, M. S.; Maskaev, A. V.; Zhdankin, V. V. *ARKIVOC* **2011**, 370–409.
6. Silva Jr., L. F.; Olofsson, B. *Nat. Prod. Rep.* **2011**, *28*, 1722–1754.
7. Zhdankin, V. V. *Hypervalent Iodine Chemistry: Preparation, Structure, and Synthetic Applications of Polyvalent Iodine Compounds*; Wiley: Chichester, U.K., **2013**.
8. Olofsson, *Topics in Curr. Chem.* **2015**, *373*, 135-166.
9. Selected examples: (a) Aradi, K.; Tóth, B. L.; Tolnai, G. J.; Novák, Z. *Synlett* **2016**, *27*, 1456-1485.
10. Ryan, J. H.; Stang, P. J. *Tetrahedron Lett.* **1997**, *38*, 5061-5064.
11. Phipps, R. J.; Grimster, N. P.; Gaunt, M. J. *J. Am. Chem. Soc.* **2008**, *130*, 8172-8174.
12. Phipps, R. J.; Gaunt, M. J. *Science* **2009**, *323*, 1593-1597.
13. Bigot, A.; Williamson, A. E.; Gaunt, M. J. *J. Am. Chem. Soc.* **2011**, *133*, 13778-13781.;
14. Allen, A. E.; MacMillan, D. W. C. *J. Am. Chem. Soc.* **2011**, *133*, 4260-4263.
15. Phipps, R. J.; Mc Murray, L.; Ritter, S.; Duong, H. A.; Gaunt, M. J. *J. Am. Chem. Soc.* **2012**, *134*, 10773-10776.
16. Xu, Z.-F.; Cai, C.-X.; Liu, J.-T. *Org. Lett.* **2013**, *15*, 2096-2099.

17. Suero, M. G.; Bayle, E. D.; Collins, B. S. L.; Gaunt, M. J. *J. Am. Chem. Soc.* **2013**, *135*, 5332-5335.
18. Walkinshaw, A. J.; Xu, W.; Suero, M. G.; Gaunt, M. J. *J. Am. Chem. Soc.* **2013**, *135*, 12532-12535.
19. Casitas, A.; Ribas, X. *Chem. Sci.* **2013**, *4*, 2301-2318.
20. Cahard, E.; Bremeyer, N.; Gaunt, M. J. *Angew. Chem. Int. Ed.* **2013**, *52*, 9284-9288.
21. Peng, J.; Chen, C.; Chen, J.; Su, X.; Xi, C.; Chen, H. *Org. Lett.* **2014**, *16*, 3776-3779.
22. Fañanás-Mastral, M.; Feringa, B. L. *J. Am. Chem. Soc.* **2014**, *136*, 9894-9897.
23. Buksnaitienė, R.; Cikotienė, I. *Synlett* **2015**, *26*, 479-483.
24. Cahard, E.; Male, H. P. J.; Tissot, M.; Gaunt, M. J. *J. Am. Chem. Soc.* **2015**, *137*, 7986-7989.
25. Beaud, R.; Phipps, R. J.; Gaunt, M. J. *J. Am. Chem. Soc.* **2016**, *138*, 13183-13186.
26. Teskey, C. J.; Soheli, S. M. A.; Bunting, D. L.; Modha, S. G.; Greaney, M. J. *Angew. Chem. Int. Ed.* **2017**, *56*, 5263-5266.
27. Fañanás-Mastral, M. *Synthesis* **2017**, *49*, 1905-1930.
28. Kumar, D.; Arun, V.; Piliandhi, M.; Mehra, M. K.; Khandagale, S. B. *Chem. Biol. Interface*, **2016**, *i*, 270-281.
29. Cao, C. K.; Sheng, J.; Chen, C. *Synthesis* **2017**, *49*, 5081-5092.
30. Zhang, F.; Das, S.; Walkinshaw, A. J.; Casitas, A.; Taylor, M.; Suero, M. G.; Gaunt, M. J. *J. Am. Chem. Soc.* **2014**, *136*, 8851-8854.
31. Li, X.; Xu, J.; Zhang, P.; Gao, Y.; Wu, J.; Tang, G.; Zhao, Y. *Synlett* **2014**, *25*, 2009-2012.
32. Yang, Y.; Han, J.; Wu, X.; Mao, S.; Yu, J.; Wang, L. *Synlett* **2014**, *i*, 1419-1424.

33. Shi, L.; Wang, Y.; Yang, H.; Fu, H. *Org. Biomol. Chem.* **2014**, *12*, 4070-4073.
34. Pang, X.; Chen, C.; Su, X.; Li, M.; Wen, L. *Org. Lett.* **2014**, *16*, 6228-6231.
35. Pang, X.; Lou, Z.; Li, M.; Wen, L.; Chen, C. *Eur. J. Org. Chem.* **2015**, *15*, 3361-3369.
36. Yang, Y.; Han, J.; Wu, X.; Xu, S.; Wang, L. *Tetrahedron Lett.* **2015**, *56*, 3809-3812.
37. Wu, X.; Yang, Y.; Han, J.; Wang, L. *Org. Lett.* **2015**, *17*, 5654-5657.
38. Minami, H.; Suead, T.; Okamoto, N.; Miwa, Y.; Ishikura, Y.; Yanada, R. *Eur. J. Org. Chem.* **2016**, *3*, 541-548.
39. Oh, K. H.; Kim, J. G.; Park, J. K. *Org. Lett.* **2017**, *19*, 3994-3997.
40. Wang, Y.; Chen, C.; Peng, J.; Li, M. *Angew. Chem. Int. Ed.* **2013**, *52*, 5323-5327.
41. Aradi, K.; Bombicz, P.; Novák, Z. *J. Org. Chem.* **2016**, *81*, 920-931.
42. Sinai, Á.; Mészáros, Á.; Gáti, T.; Kudar, V.; Palló, A.; Novák, Z. *Org. Lett.* **2013**, *15*, 5654-5657.
43. Chi, Y.; Yan, H.; Zhang, W.-X.; Xi, Z. *Org. Lett.* **2017**, *19*, 2694-2697.
44. Sinai, Á.; Vangel, D.; Gáti, T.; Bombicz, P.; Novák, Z. *Org. Lett.* **2015**, *17*, 4136.
45. Stirling, A.; Nair, N. N.; Lledós, A.; Ujaque, G. *Chem. Soc. Rev.* **2014**, *43*, 4940-4952.
46. Frisch, M. J. et al. Gaussian 09, Revision E.01, Gaussian, Inc., Wallingford CT, 2013.
47. Zhao, Y.; Truhlar, D. G. *Theor. Chem. Acc.* **2008**, *120*, 215-241.
48. Marenich, A. V.; Cramer, C. J.; Truhlar, D. G. *J. Phys. Chem. B*, **2009**, *113*, 6378-6396.